NUCLEAR ENGINEERING

MASSACHUSETTS INSTITUTE OF TECHNOLOGY

NARROW CHANNEL TURBULENCE MODELING PROJECT
FINAL REPORT MITNE-299
March 1992

by: J.E. Meyer, S.M. Kwak, and T.D. Shubert
MIT Department of Nuclear Engineering

for: Oak Ridge National Laboratory
operated by Martin Marietta Energy Systems Inc.
cognizant engineer A.E. Ruggles

NARROW CHANNEL TURBULENCE MODELING PROJECT
FINAL REPORT MITNE-299
March 1992

by: J.E. Meyer, S.M. Kwak, and T.D. Shubert
MIT Department of Nuclear Engineering

for: Oak Ridge National Laboratory
operated by Martin Marietta Energy Systems Inc.
cognizant engineer A.E. Ruggles

TABLE OF CONTENTS

Section 1: PROJECT OBJECTIVES

A significant design and safety consideration for the Advanced Neutron Source Reactor (ANSR) is the possibilty that the inlet to a coolant channel becomes partially blocked by debris. Such blockage is a potential cause for fuel plate damage by distortion and/or excessive oxidation.

This project is part of an effort to establish the minimum blockage size that would cause fuel element damage. The work is aimed at turbulence modeling of the heated flow of water through a single ANSR coolant channel. The modeling uses the FLUENT computational fluid dynamics (CFD) software developed by Creare (Ref F-1).

Relevant experimental results are available for validation of calculated results. The experiment was part of the University of Minnesota doctoral research of N. Cur (ref C-1, 1982). The experiment uses turbulent air flow to cause sublimation of napthalene walls. This mass transfer can be used to provide heat transfer information by use of analogy concepts. The heat transfer information can be used to evaluate FLUENT program results.

Section 2: BACKGROUND AND GENERAL DESCRIPTIONS

2.1 AN ANSR CHANNEL

Each ANSR coolant channel is bounded on the sides by two curved (involute shaped) fuel plates and on the edges by portions of two supporting cylinders. The channel thickness is constant. A heavy water (D_2O) coolant is employed.

2.2 A RECTANGULAR CHANNEL WITH WATER FLOW

A rectangular channel has been defined for use in the FLUENT calculations. It has thermal-hydraulic characterisics that are similar to an ANSR channel but are simpler to use in turbulence modeling calculations. The channel has a thickness of 1.27 mm, a width of 84 mm, and a length of 500 mm. The flow enters from a rectangular approach passage with a thickness of 2.54 mm, a width of 84mm, and a length of 250 mm. The transition in flow area from the approach passage to the channel is smoothed in the thickness direction by a radius of 0.6 mm.

A light water (H_2O) coolant is employed. The coolant enters the channel at a low temperature (49°C), at a moderately high pressure (3.2 MPa), and at a channel average velocity of 25 m/s for an unblocked case. A constant heat flux of 6.0 MW/m^2 is applied over both sides of the channel. These conditions give a Reynolds Number of 110000 just inside the channel inlet and a Reynolds Number of 210000 just inside the channel exit.

A range of blocked cases is required in order to define plate damage limits. The flow in each blocked case is to be selected to give the same pressure at the inlet to the approach passage (and at the exit from the channel) as exists in the unblocked case. The heat flux in each blocked case is considered to be the same as in the unblocked case. In this study, only one blocked water flow case is completed. This case is based on the same flow as an unblocked counterpart rather than the same pressure drop. This single case can be considered as a trial calculation to be studied (and modified if appropriate) prior to planning the range of blocked cases.

2.3 A RECTANGULAR CHANNEL WITH AIR FLOW

Results from the doctoral research of N. Cur (refs C-1 and S-1) provide experimental data on air flow through a rectangular channel with and without blockage. Comparisons of FLUENT results with these experimental data should aid in estimating the confidence to be placed on the FLUENT water flow calculations.

The Sparrow and Cur channel has a thickness of 4.45 mm, a width of 81.3 mm, and a length of 185 mm. The air enters from a large plenum region at atmospheric pressure. Channel average velocities from 11 m/s to 54 m/s are employed for the tests. These conditions give a Reynolds Number in a range from 6000 to 30000. Information on local heat transfer coefficients is

obtained from mass transfer data and from analogy reasoning. The channel faces for the mass transfer tests are constructed of cast napthalene.

The blocked cases have 25% and 50% blockages located at the edge of the channel. That is, the thickness of the channel is completely closed at the entrance for 25% and 50% of the width. In the present study, calculations are completed for two air flow cases at a Reynolds number of 30000, one unblocked and the second blocked for 25% of the width.

2.4 DETAILS OF THE CALCULATED CASES

Four combinations of fluid, geometry, and operating conditions have been studied with FLUENT, as indicated in Table 2-1:

TABLE 2-1: CASES SELECTED FOR FLUENT CALCULATIONS

Section	Channel Geometry and Fluid	Blockage Amount (%)	Blockage Position	Pressure or Flow Boundary Condition	Channel Inlet Reynolds Number
§3	Air	zero	---	P-Bdy	31100
§4	Air	25	edge	P-Bdy	
§5	H_2O	zero	---	V-in	110000
§6	H_2O	10	central	V-in	110000

Notes:

- for fluid = "air," the channel has: thickness = 4.45 mm; width = 81.3 mm; length = 185 mm; and hydraulic equivalent diameter = 8.43 mm.
- for fluid = "H_2O," the channel has: thickness = 1.27 mm; width = 84.0 mm; length = 500 mm; and hydraulic equivalent diameter = 2.50 mm.
- the boundary condition denoted by "P-Bdy" uses a special treatment of plenum pressures provided in FLUENT and described in §3.2.
- the boundary condition denoted by "V-in" is implemented by requiring that the FLUENT solution be based on a spatially uniform inlet velocity provided as part of the input.
- all cases are performed with heat addition and with a k-ϵ turbulence model.

2.5 COORDINATES, BLOCKAGES, TRAVERSES

The notation adopted for coordinate axes used in this report is shown schematically in fig 2-1. The orientation of the channel is that used in illustrations in the Cur thesis.

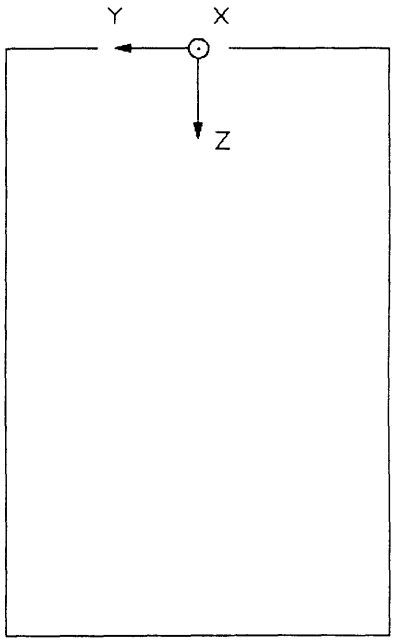

Figure 2-1.
Coordinate Axes Used to Identify Locations

The net fluid flow is in the positive z-direction (also designated the axial direction and the length direction). The channel extends in the z-direction from z = 0 (the inlet) to z = L (the exit); where L is the channel length.

The channel width direction is the y-direction. W denotes the channel width. The origin of the y-axis is in the center of the width; the channel extends from y = - W/2 to y = + W/2.

The channel thickness direction is the x-direction. t denotes the channel thickness. The origin of the x-axis is in the center of the width; the channel extends from x = - t/2 to x = + t/2.

There is no explicit modeling of the approach passage geometry. However, where appropriate, we have used an area ratio to represent that geometry. The area ratio (β) is defined as the channel flow area divided by the approach passage flow area. β is zero for the air flow cases and 0.5 for the water flow cases.

The 25% edge blockage in the blocked air flow case extends from y = + W/4 = 20.3 mm to + W/2 = + 40.6 mm. The 10% center blockage in the blocked water flow case extends from y = - W/20 = - 4.2 mm to y = + W/20 = + 4.2 mm.

Four traverses at specified y-coordinate values have been used for providing information in each channel type (air or water). The traverse positions are based on blockage locations. Traverses 1, 2, and 3 are equally spaced from the edge of the FLUENT calculation domain (the edge is at y = + W/2 for air flow cases and at y = 0 for the symmetric water flow calculation). The blockage extends in FLUENT from this edge to a position midway between traverse 2 and traverse 3. Traverse 4 is in the open portion of the channel inlet half of the distance from the edge of the blockage to the edge of the channel. Explicit y-coordinates of interest are provided in table 2-2:

TABLE 2-2: Y-COORDINATES FOR BLOCKAGES AND TRAVERSES

Case	Blockage Edge by Opening	Traverses 1	2	3	4
Air	+ 20.3	+ 32.5	+ 24.4	+ 16.3	- 10.2
Water	+ 4.2	+ 1.7	+ 3.4	+ 5.0	+ 18.9

Notes:

- y-coordinates (mm) are based on the coordintate system of fig 2-1.
- additional information is supplied in the text.
- the indicated traverse locations are used for both blocked and unblocked cases.

2.6 PREPARATION OF FLUENT INPUT

The following input information has been prepared for use in the FLUENT studies:

- Fluid Properties: Polynomial relations have been developed for both water and air in the thermal-hydraulic operating range required for the cases of Table 1-1. Data from refs K-1, K-2, and P-1 were employed in constructing the polynomials.

- Mesh Sizes: The FLUENT report (Ref F-1) provides recommendations for mesh size selection. We have selected mesh intervals based on these recommendations but subject also to computing time and storage restrictions. The resulting selections of mesh intervals within the channels are as follows (additional mesh intervals are required to represent boundary conditions but are not detailed here):

  For the air flow cases:

  10 mesh intervals of 0.2225 mm are used in the x-direction (from x = 0 to x = 2.225 mm with a symmetry condition employed at x = 0).

  40 mesh intervals of 2.03 mm are used in the y-direction (from y = - 40.65 mm to y = 40.65 mm).

  40 mesh intervals are used in the z-direction. The interval is 0.2831 mm at the inlet and expands by a constant factor (1.114) until it reaches 19.34 mm adjacent to the exit.

For the water flow cases:

10 mesh intervals of 0.0635 mm are used in the x-direction (from x = 0 to x = 0.635 mm with a symmetry condition employed at x = 0).

45 mesh intervals mm are used in the y-direction (from y = 0 to y = 42 mm with a symmetry condition employed at y = 0). The mesh intervals are uniform at 0.42 mm between y = 0 and y = 4.2 mm; they then increase by a constant factor (1.176) until reaching 3.23 mm near y = 20.8 mm; and finally decrease by a constant factor (0.833) until reaching 0.0664 mm next to the wall at the channel edge.

42 mesh intervals are used in the z-direction. The interval is 0.0634 mm at the inlet and expands by a constant factor (1.19) until it reaches a value of 80 mm adjacent to the exit.

- Inlet Boundary Conditions: We have calculated an appropriate fully developed velocity profile for use at the entrance to the approach passage for the water flow cases. We have also obtained information to represent the turbulent intensity distribution for the entering flow (adapting information from Hinze, Ref. H-1). These details were not used for the final FLUENT problem since there is no explicit treatment of the approach passage.

Section 3: UNBLOCKED AIR FLOW CASE

3.1 CUR EXPERIMENTS

As indicated above, local mass transfer data were obtained during the Cur experiments (Refs C-1 and S-1) from measured sublimation depths. Each mass transfer result is expressed by Cur in terms of a Sherwood number (Sh):

$$Sh = K D_e / \mathcal{D} \quad ; \tag{3-1}$$

where K is a mass transfer coefficient (m/s); D_e is the channel equivalent hydraulic diameter (m); and $\mathcal{D}$ is the napthalene-air diffusion coefficient (m^2/s).

The diffusion coefficient for interpreting the Cur experiments is obtained on the basis of a known Schmidt number (Sc) for the napthalene-air system:

$$Sc = \nu / \mathcal{D} = 2.5 \quad ; \tag{3-2}$$

where ν is the air kinematic viscosity (m/s^2).

Each Sherwood number can be converted to a corresponding Nusselt number by using an analogy between mass transfer and heat transfer (Ref C-1, p. 39):

$$Nu = (Pr / Sc)^n Sh \quad ; \tag{3-3}$$

where $Nu = h D_e / k$ denotes the Nusselt number, with h = a convective heat transfer coefficient ($W/(m^2 \bullet K)$) and with k = the thermal conductivity of the air ($W/(m \bullet K)$);

where $Pr = c_p \mu / k = 0.714$ denotes the Prandtl number for air, with c_p = the specific heat of the air at constant pressure ($J/(kg \bullet K)$) and with μ = the viscosity of the air ($Pa \bullet s$); and

where n is an exponent (here 0.4) that depends on the correlation adopted to obtain Prandtl number dependence.

For the calculations of this report (with the Schmidt number, the Prandtl number, and the exponent taken to be, respectively, 2.5, 0.714, and 0.4), eq 3-3 becomes:

$$Nu = 0.606\, Sh \quad . \tag{3-4}$$

Equation 3-4 is therefore available to obtain heat transfer information from the Cur experiments. However, there remain some concerns about the adequacy of the analogy between heat transfer and mass transfer. There is also a question that arises from the nature of the wall boundary conditions that describe the transfer processes. The experiments simulated a constant wall temperature heat transfer process whereas the ANSR application is better

approximated by a constant heat flux. We chose to do all calculations (hand and FLUENT) on the basis of constant heat flux. The calculations therefore differ from the Cur experiments in two significant respects: heat transfer rather than mass transfer; and constant heat flux rather than constant wall temperature. The magnitude of errors so introduced is unknown. We should, in some sense, obtain a feel for the combined effects caused by the mass transfer analogy and by the constant heat flux boundary condition. The heated channel that has been chosen for these calculations is discussed in §3.2.

3.2 FLUENT HEATED CHANNEL REPRESENTATION

The thickness, width, and length dimensions for the channel are the same as those for the Cur experiment (see §2.3). However, our attempts to model flow in the large approach passage explicitly produced non-converging FLUENT problems. We therefore adopted the pressure boundary approach of Tutorial 23, Ref F-1. In this approach, pressures are specified for an inlet plenum and for an exit plenum. For each cell adjacent to the inlet, the fluid pressure is set equal to the specified inlet plenum pressure minus one dynamic head (calculated). For each cell adjacent to the exit, the fluid pressure is set equal to the specified exit plenum pressure.

This approach introduces some artificial constraints in the vicinity of the channel inlet. Velocity conditions in this region may not be well represented in the FLUENT calculations. In particular, errors may be introduced in the direction of the velocity vector and in the turbulence intensity. A good treatment of these details is especially desirable for cases with blockage; however, we have not yet found a practical remedy for these inlet region errors. The pressure boundary approach has been adopted to obtain calculated results which at least provide for treating other important features of the flow.

This pressure boundary method of defining channel hydraulic conditions requires that pressures in the inlet and exit plenum be user specified. The flowrate is therefore obtained as a result of the FLUENT solution process. Values were used for inlet plenum pressure (101.3 kPa) and for exit plenum pressure (3.16 kPa lower) to obtain approximately 30000 for the channel Reynolds number ($Re = \rho V_m D_e / \mu$; where ρ is the density of the air; and where V_m is the average air velocity). The chosen pressures give V_m = 56.3 m/s inside the channel at the inlet and Re values of 31100 and 30300 at the inlet and exit, respectively.

As indicated above, we have chosen to specify a constant heat flux in our FLUENT analyses of the air experiments. The specified heat flux must be large enough to obtain a significant difference between wall temperatures and bulk temperatures. It must also be small enough to avoid large bulk temperature changes. We have adopted a heat flux of 9.31 kW/m^2. This, for the zero blockage case, gives a bulk temperature rise of approximately 12 K and a difference between the wall temperature and the bulk temperature of approximately 40K. We have also chosen an inlet plenum temperature of 20°C to provide air temperatures likely to be close to the Cur conditions.

3.3 HAND CALCULATIONS

There are conventional simple calculations to describe heat transfer and fluid flow in the channel of §3.2. These are designated "hand calculations" although they actually were executed using Mathcad and Lotus 123 software. Calculation results include bulk temperature (T_B), wall temperature (T_W), and air pressure (p) as a function of axial position (z). Equations are as follows:

The bulk temperature is taken from the bulk enthalpy (H_B) by use of the following equation and the use of fluid property information:

$$H_B = H_I + \int_0^z \frac{P_h q''}{G A_F}\, dz - \frac{1}{2} V_m^2 \quad ; \tag{3-5}$$

where H_I denotes the inlet plenum enthalpy; q'' is the heat flux; P_h is the heated perimeter; $G = \rho V_m$ is the mass velocity; A_F is the flow area; the last term on the right hand side is an adjustment for stagnation enthalpy considerations; and the velocity in the inlet plenum is taken as zero.

The wall temperature is obtained from:

$$T_W = T_B + \frac{q''}{h} \quad ; \tag{3-6}$$

where the heat transfer coefficient h is taken from the following Nusselt number relation:

$$Nu = (0.023\, Re^{0.8}\, Pr^{0.4}) \left(1 + \frac{0.58\, D_e}{z}\right) \quad . \tag{3-7}$$

The first parenthesis pair on the right hand side of eq 3-7 contains the familiar Dittus-Boelter relation for fully developed Nusselt number calculations. The second parenthesis pair contains an adjustment for the developing region near the channel inlet. This adjustment function was obtained to represent a handbook graph (Re = 30000, Pr = 0.73, fig 24, p 7-33, ref R-1).

The pressure as a function of z is given by:

$$p = p_I - \int_0^z \frac{f}{D_e} \frac{G^2}{2\rho}\, dz - (K_c + 1 - \beta^2) \frac{G^2}{2\rho_o} \quad ; \tag{3-8}$$

where K_c is the contraction loss coefficient; β is the ratio of channel area to inlet plenum area (zero for the calculations of this section); ρ_o is the fluid density at $z = 0$; and f is a friction

factor obtained from:

$$f = \left(\frac{0.184}{Re^{0.2}}\right)\left(\frac{\mu_w}{\mu}\right)^{0.35} \quad . \tag{3-9}$$

The first parenthesis pair on the right hand side of eq 3-9 contains a commonly used relation for isothermal friction factor. The second parenthesis pair contains an adjustment for heating effects suggested by Dormer (ref D-1). This adjustment employs the ratio of fluid viscosity at the wall to bulk viscosity.

3.4 RESULTS OF CALCULATIONS

Three calculated temperatures as a function of axial position are shown in the fig 3-1:

The upper curve (symbol o) gives the FLUENT wall temperatures. The curve shows effects of developing heat transfer with a dip in wall temperature in about the first 40 mm of the channel of the channel length.

The lower curve (symbol x) gives the FLUENT air temperatures at the thickness centerline (x = 0) along traverse 4 (y = -10.2 mm. Note that there is very little heating of the air that flows at x = 0 until the axial level z = 80 mm is passed.

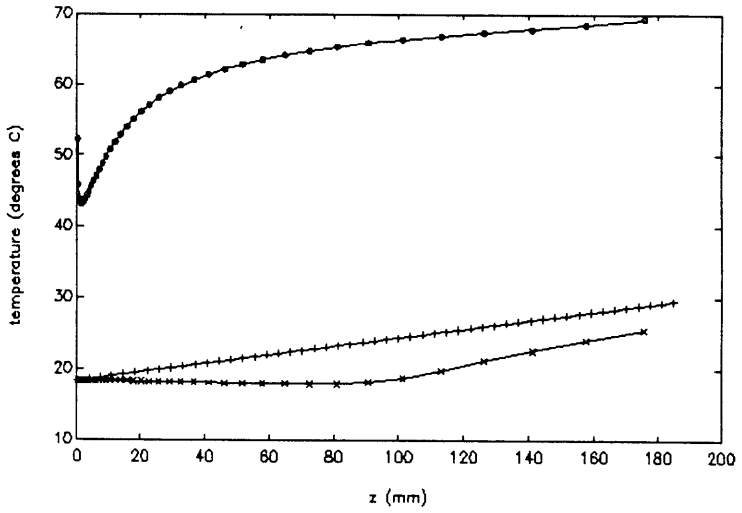

Figure 3-1. Temperatures Vs Axial Position; Unblocked Air Flow Case (traverse 4)
—o— FLUENT T-wall
—x— FLUENT T-air (x = 0)
—+— T-bulk (hand)

The remaining curve (symbol +) is a hand calculation of the bulk temperature. It is roughly linear since the specific heat is nearly constant. Note that the air temperature at z = 0 is about 18°C (below the plenum temperature of 20°C) and reflects the effects of the stagnation term in eq 3-5.

Nusselt numbers for Cur, FLUENT, and hand are illustrated in fig 3-2. The Cur curve is taken from eq 3-4 and from fig 4.8, p 56, ref C-1 using the curve for spanwise-average, Re = 30000, and zero blockage.

All curves in fig 3-2 have a similar shape. They also agree in magnitude fairly well (within 8%) in the asymptotic region (z > 150 mm). All curves show a region of enhanced heat transfer as the flow develops after entry into the channel. The hand calculations (eq 3-7) show a continuously increasing Nu as z approaches 0. Both of the other curves show an early region of diminished Nu prior to the developing enhancement.

The FLUENT peak value of Nu is significantly lower than the other two, indicating an underprediction of the developing region effect (however, behavior within that region that is qualitatively correct).

Axial pressure distribution curves are displayed in fig 3-3. The FLUENT curve represents all four traverses well. The Cur values are taken from fig 10, p 534, ref C-1 using the curve for Re = 30000 and zero blockage.

The three curves show essentially the same behavior except for the pressure change upon entry into the channel. Each of

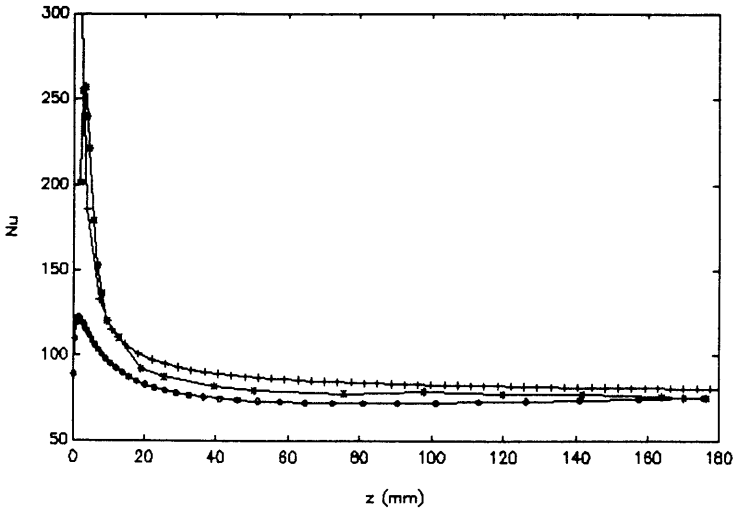

Figure 3-2. Nusselt Number Vs Axial Position; Unblocked Air Flow Case
—o— FLUENT
—*— Cur experiment
—+— hand calc

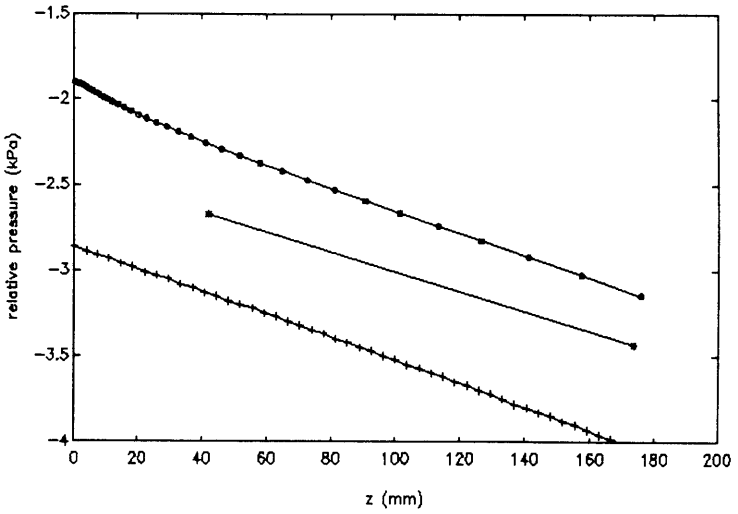

Figure 3-3. Pressure ($p - p_I$) Vs Axial Position; Unblocked Air Flow Case
—o— FLUENT
—*— Cur experiment
—+— hand calc

the three has a value at z = 0 that is lower than the plenum pressure because of the recoverable pressure change (acceleration). This change is the $(1 - \beta^2) \frac{G^2}{2 \rho_o}$ portion of the last term in eq 3-8 and amounts to about 1.9 kPa. The observed differences in the curves can be considered to result from differences in the contraction loss. The effective values of K_c are (0, 0.3, and 0.5) for FLUENT, Cur, and hand, respectively. The FLUENT value is artificial and is part of the pressure boundary method of describing channel flow conditions. The hand value is based on an abrupt contraction (table 6-7, ref B-1). The Cur value is based on his experiment with the possibility of enough rounding at the entrance to reach 0.3.

The results that have been displayed in this chapter indicate that calculations based on FLUENT, Cur, or hand can provide a reasonable description of the unblocked air flow case.

Section 4: BLOCKED AIR FLOW CASE

4.1 HEAT TRANSFER COEFFICIENTS AND NUSSELT NUMBERS

Many of the comments and equations of section 3 also apply here. However, it seems important to express some thoughts about interpreting calculated temperatures to obtain heat transfer coefficients (and subsequently Nusselt numbers) in two-dimensional flow situations.

In particular, the two-dimensional (2-d) flow situations of interest occur in rectangular channels with swirls (including negative axial velocities) caused by inlet blockage. Such flow patterns are actually three-dimensional but the major features can be described using velocity components in two-dimensions (y and z). Similarly, the unblocked case of section 3 is designated as one-dimensional (1-d, z-direction) in the present discussion.

A definition for the heat transfer coefficient h can be obtained by rearranging eq 3-6 to obtain:

$$h = \frac{q''}{T_W - T_B} \quad . \tag{4-1}$$

The heat flux (q'') and the wall temperature (T_W) are interpreted to be evaluated at a local y,z position[1] in either 1-d or 2-d. The bulk temperature (T_B) is, however, a temperature that corresponds to a flow-weighted or mixing-cup enthalpy (H_B) which is defined in terms of an integral over the flow area:

$$H_B = \frac{1}{G A_F} \int_{A_F} \rho V H \, dA \quad ;$$

where ρ, V, and H denote local values (within the flow area) of density, axial component of velocity, and enthalpy.

The bulk enthalpy and thus the bulk temperature can be obtained from a 1-d axial energy balance (even in 2-d applications). We feel that this bulk temperature and eq 4-1 should be used to calculate the heat transfer coefficient. Therefore, in the swirl case, the heat transfer coefficient for a point within the swirl reflects the effects of both a reduced velocity and a fluid temperature that may be significantly higher than the bulk temperature. This treatment is consistent with that of Cur (eqs 5 and 15, ref C-1). The treatment is a practical one in that appropriate Nusselt numbers from multi-dimensional calculations (or from experiments) can be combined with simple 1-d calculations to estimate blockage effects.

---

[1] This study makes no attempt to quantify, in either 1-d or 2-d, wall temperatures near the edges of the channel (i.e., near y = ± W/2).

4.2 VELOCITY DISTRIBUTIONS

FLUENT calculations applied to the blocked air flow case show a swirl existing behind the blockage, as displayed in fig 4-1:

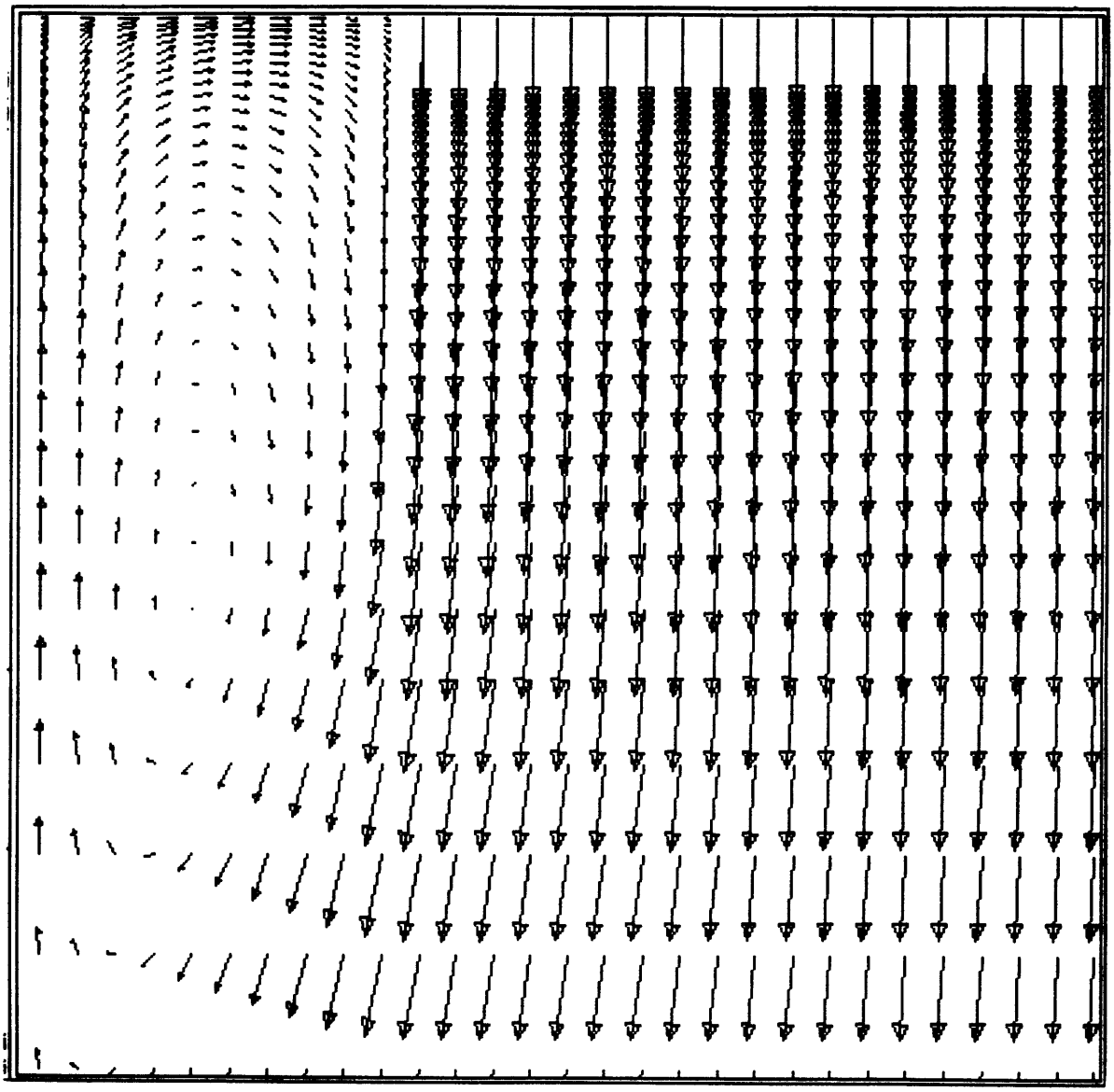

Figure 4-1. Air Velocity Vectors (from FLUENT) Blocked Air Flow Case
y from + 41 mm to - 19 mm
z from 0 to + 60 mm

The orientation of fig 4-1 is taken from fig 2-1; that is, the z-axis (flow direction) is directed downward on the page and the y-axis is directed to the left on the page.

In fig 4-2, the blocked air flow pattern from FLUENT is compared to that obtained in the Cur experiments (fig 4.4, p 50, ref C-1):

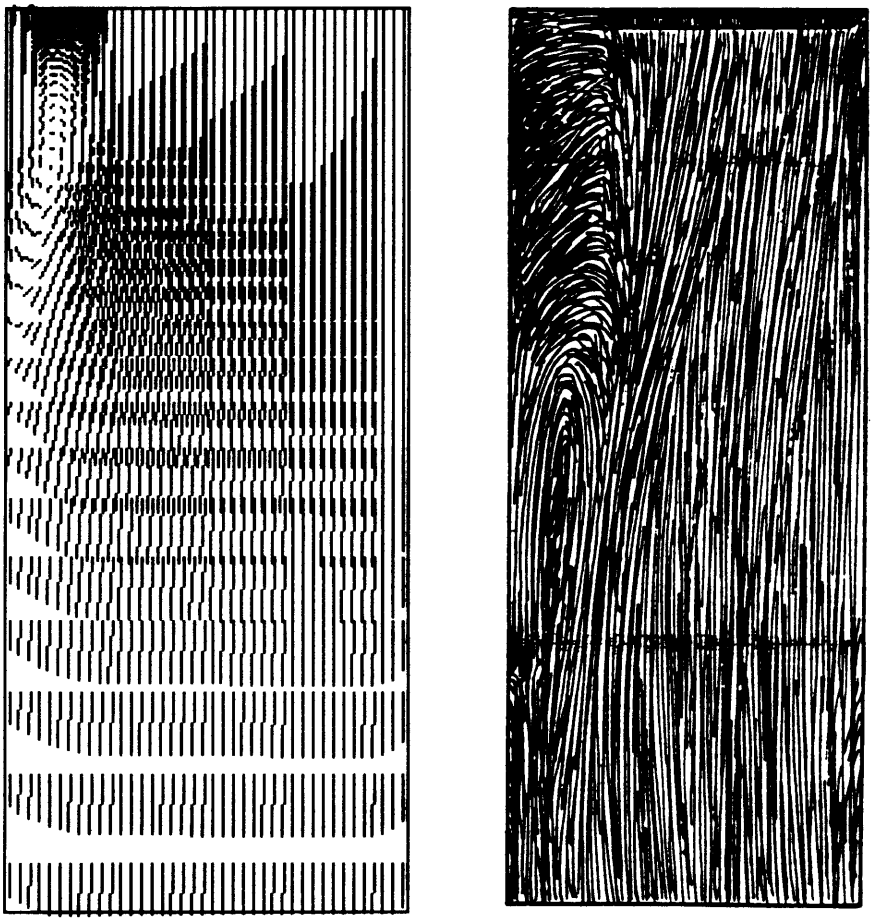

Figure 4-2. Blocked Air Flow Patterns
pattern from FLUENT on left
pattern from Cur (ref C-1) on right
full y,z domain displayed

The orientation of fig 4-2 is taken from fig 2-1; that is, the z-axis (flow direction) is directed downward on the page and the y-axis is directed to the left on the page.

The size of the FLUENT swirl is roughly 20 mm by 60 mm with the center at z = + 30 mm. The Cur swirl is much larger (roughly 20 mm by 160 mm with the center at z = + 110 mm). This is a major disagreement. The persistence of the Cur swirl implies that heat transfer degradation also persists for a much greater distance from the inlet than indicated by the FLUENT results.

4.3 TEMPERATURES

The results of FLUENT wall temperature calculations are portrayed in figs 4-3 through 4-6 corresponding, respectively, to traverses 1 through 4. The air temperature at x = 0 is also shown for each traverse.

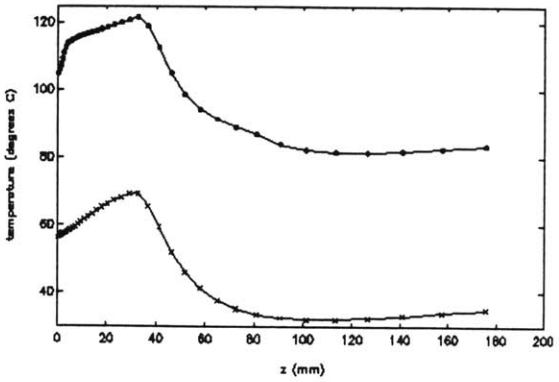

Figure 4-3. Wall Temperature and Air Temperature (x = 0); Blocked Air Flow Case (Tr 1).

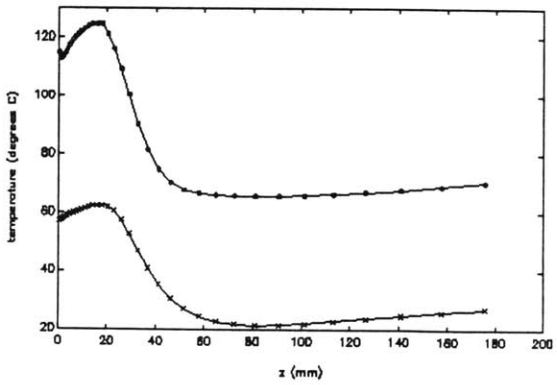

Figure 4-4. Wall Temperature and Air Temperature (x = 0); Blocked Air Flow Case (Tr 2).

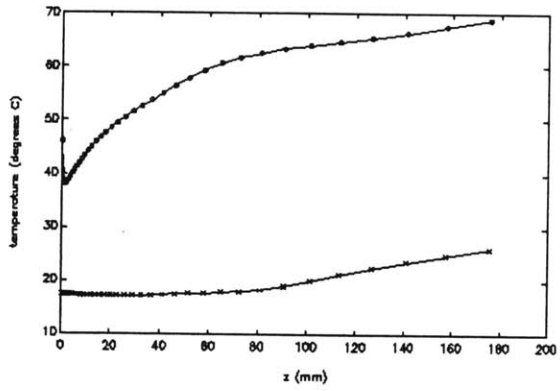

Figure 4-5. Wall Temperature and Air Temperature (x = 0); Blocked Air Flow Case (Tr 3).

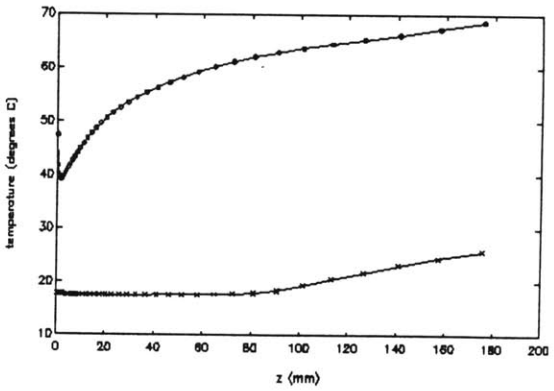

Figure 4-6. Wall Temperature and Air Temperature (x = 0); Blocked Air Flow Case (Tr 4).

Traverses 3 and 4 are clear of the blockage and behave essentially the same as the unblocked case of fig 3-1.

Traverses 1 and 2 are behind the blockage. For these traverses and for the region within the swirl (approximately 60 mm long), the temperature of both

air and wall are elevated above the corresponding temperatures beyond the swirl. Traverse 1 remains somewhat elevated for the entire channel.

4.4 NUSSELT NUMBERS

Figures 4-7 through 4-10 display Nusselt numbers obtained from Cur[2]. The Cur values are compared to Nusselt numbers obtained from the FLUENT wall temperatures of figs 4-3 through 4-6, from the bulk temperature of fig 3-1, and from eq 4-1:

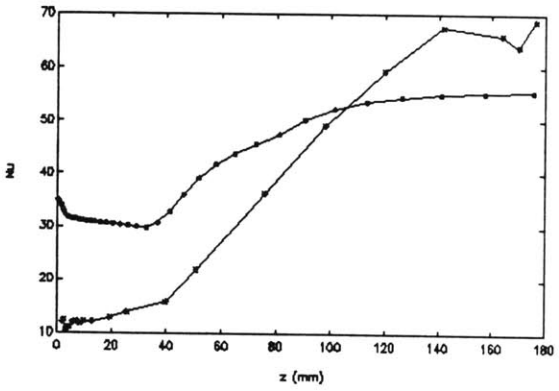

Figure 4-7. Nusselt Numbers for Blocked Air Flow Case (Tr 1); —o— FLUENT; —*— Cur

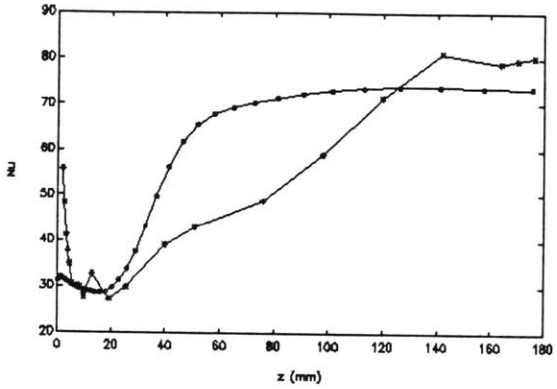

Figure 4-8. Nusselt Numbers for Blocked Air Flow Case (Tr 2); —o— FLUENT; —*— Cur

The first two of the Nusselt number figures are for the traverses behind the blockage and, in many portions, within the swirl. The figures for traverses 3 and 4 represent regions outside of the blockage and outside of the swirl. Comments include:

- All results are lower than the unblocked air results of fig 3-2 (although the unblocked results are approached as z becomes large).
- The Cur results are especially low for traverse 1 near z = 0; the FLUENT counterparts are on the order of triple the Cur results.
- The dip in all curves seems to recover before the traverse leaves the swirl. The recovery seems to come relatively sooner for the Cur results
- The Nusselt number figures for traverses 3 and 4 show essentially the same behavior as for the unblocked air flow case (fig 3-2)

---

[2] Obtained from Eq 3-4 applied to data extracted from figs 4.25a through 4.25c, pp 108 to 110, ref C-1.

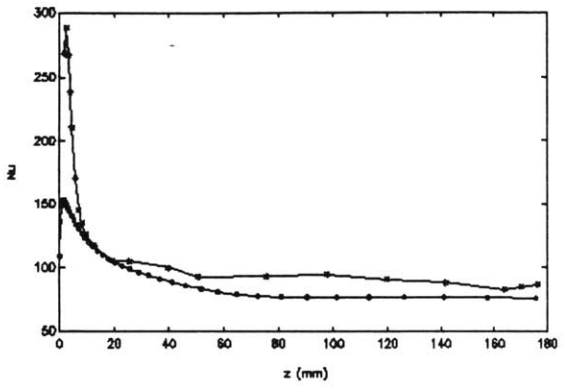

Figure 4-9. Nusselt Numbers for Blocked Air Flow Case (Tr 3);
—o— FLUENT; —*— Cur

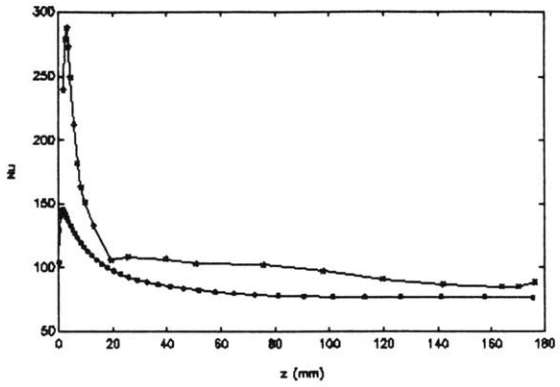

Figure 4-10. Nusselt Numbers for Blocked Air Flow Case(Tr 4);
—o— FLUENT; —*— Cur

4.5 PRESSURES

The axial pressure distributions from FLUENT for the four traverses are displayed in fig 4-11. Prominent features are the low pressure accompanying

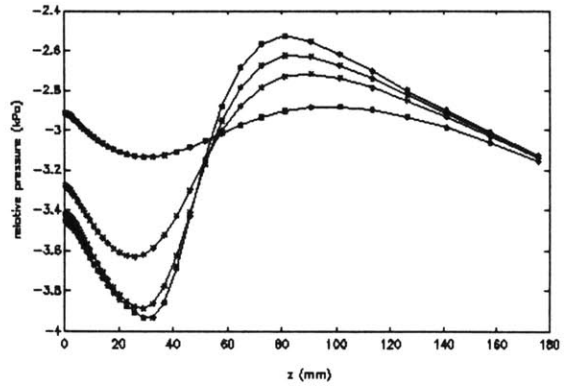

Figure 4-11. FLUENT Axial Pressure Distributions for Blocked Air Flow Case;
—*— Tr 1; —+— Tr2
—x— Tr 3; —o— Tr4

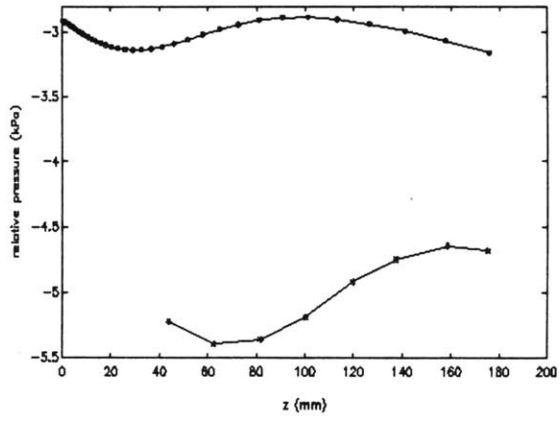

Figure 4-12. Pressure vs z for Blocked Air Flow Case
—o— FLUENT (Tr 4);
—*— Cur

the center of the swirl and the subsequent high pressure causing the flow to decelerate. These features are most prominent for traverse 1 (well behind the

blockage and are relatively mild for traverse 4 (the mid-point of the open entrance).

This traverse 4 is compared in fig 4-12 to a pressure traverse obtained from Cur[3]. The curves have a similar shape (with a dip and a subsequent hump). The dip for FLUENT occurs earlier (for a smaller value of z). This observation agrees with the smaller FLUENT swirl. The Cur curve is again below the FLUENT curve (as it was in the unblocked case, fig 3-3). However, in this blocked case, the discrepancy is much larger.

It appears that FLUENT can be used to produce a pressure distribution with the right placement of dip and hump. However, it is incorrect in magnitude and is based on an incorrect swirl size.

---

[3] Obtained from the FLUENT flowrate and from data extracted from fig 4.47, Re = 30000, 25% blockage, p 148, ref C-1.

Section 5: UNBLOCKED WATER FLOW CASE

5.1 HAND CALCULATIONS

We have completed a number of one-dimensional hand calculations to understand more completely the numbers and ranges involved. The hand calculations are performed using the equations and techniques that are summarized in §3.3. The results of our hand calculations for the water flow case include the following:

- An energy balance (eq 3-5) is used to find bulk temperature versus axial position. The bulk temperatures cover a range from the inlet at 49°C to the exit at 94°C.

- Fully developed single phase heat transfer coefficients (and adjustments for the effects of developing flow and temperature near the inlet) are obtained as expressed in eq 3-7.

- The viscosity change over the calculated bulk temperature range is very large (large enough so that the Reynolds Number about doubles). This effect is included in our calculations.

- There is a related heating effect on wall friction that is also included. The effect is represented by the second term in eq 3-9 and is caused by having fluid near the walls with a viscosity that is lower than the bulk viscosity.

- The Blevins handbook, Ref B-1, is used to estimate the entrance loss coefficient. Combining this loss information with estimates of other pressure drop components, we find that the entrance to the approach passage is at a pressure that is 73 kPa above the exit from that passage. There is a 269 kPa pressure drop across the entrance to the channel and an additional 910 kPa pressure drop from just inside the channel inlet to just inside the channel exit.

Some of the hand calculation results are used as reference curves for comparison to FLUENT output in the subsections that follow.

5.2 FLUENT HEATED CHANNEL REPRESENTATION

The full three-dimensional representation of both the approach passage and the heated channel requires too many mesh points. We were able to represent both components in two-dimensions (x, z). However, we felt that it would be preferable to have an unblocked case with the same mesh structure as the blocked case. That decision lead to the use of the FLUENT representation that follows.

All fluid mesh points are within the channel (i.e., no contraction is represented). The flow conditions at the inlet are defined by providing a uniform z-direction velocity for all inlet mesh boxes at $z = 0$.

This approach precludes FLUENT calculation of losses or acceleration upon contraction. Details of velocity vector and turbulent intensity variation upon contraction are also missing. The approach does give a practical method of studying blockage consequences.

A description of the FLUENT mesh size selection is contained in §2.6.

5.3 RESULTS OF CALCULATIONS

Three calculated temperatures as a function of axial position are shown in the fig 5-1:

The upper curve gives the FLUENT wall temperatures. The curve shows the effects of developing heat transfer (see similarities to the air results of fig 3-1).

The curve for the FLUENT water temperatures (symbol x, location at x = 0) shows an early delay in temperature penetration in a manner similar to the air results of fig 3-1.

The remaining curve is a hand calculation of bulk temperature, starting at 49°C, discharging at 94°C, and behaving roughly linearly between the extremes.

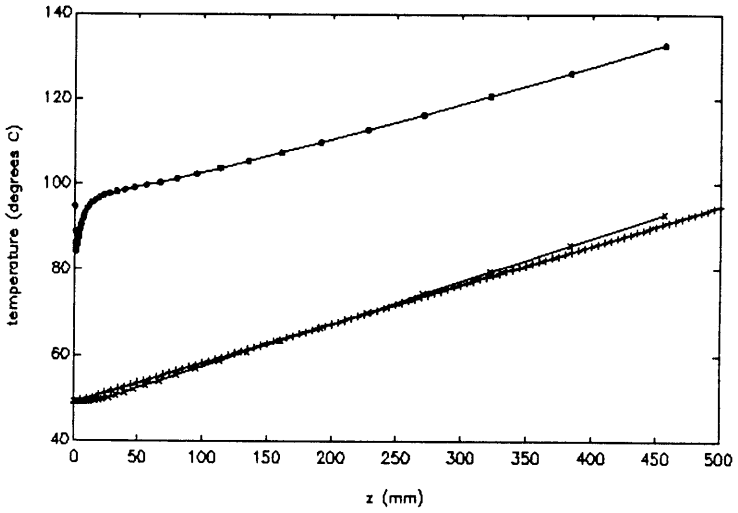

Figure 5-1. Temperatures;
Unblocked Water Flow Case (traverse 4)
—o— FLUENT T-wall
—x— FLUENT T-water (x = 0)
—+— T-bulk (hand)

Nusselt numbers for FLUENT and hand are displayed in fig 5-2. The FLUENT results, after the initial developing region, are about 18% above the hand results. This discrepancy seems large but is probably within the accuracy of the Dittus-Boelter equation used for hand calculations (eq 3-6)

Axial pressure distribution curves are displayed in fig 5-3. Both curves behave approximately linearly. There is, however, a slight curvature for the FLUENT results near the entrance (indicating a velocity developing effect).

The friction factor for FLUENT seems to be about 20% higher than the hand calculated value. This discrepancy seems too large The discrepancy could be partly removed by neglecting the adjustment for heating effects (the second parenthesis pair in eq 3-9). However, the true nature of the discrepancy is unclear and the heating effect removal seems unwarranted.

The results in this chapter indicate that the FLUENT results and the hand results behave in similar manners. Quantitative discrepancies are noted but not well explained.

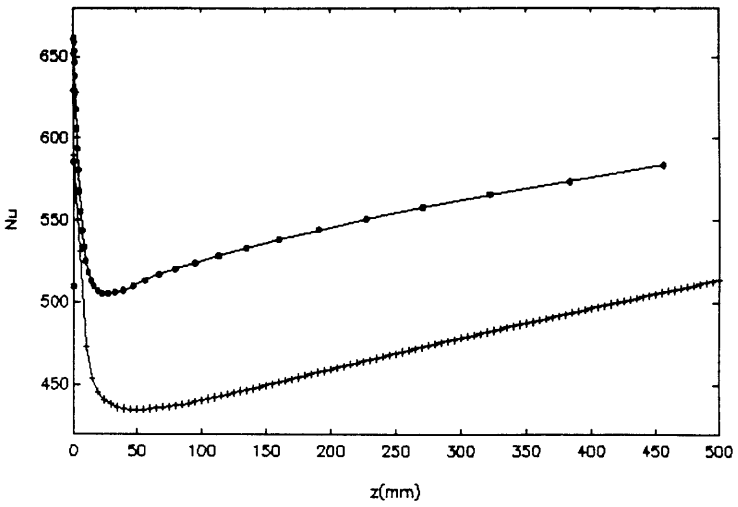

Figure 5-2. Nusselt Numbers;
Unblocked Water Flow Case
—o— FLUENT
—+— hand calc

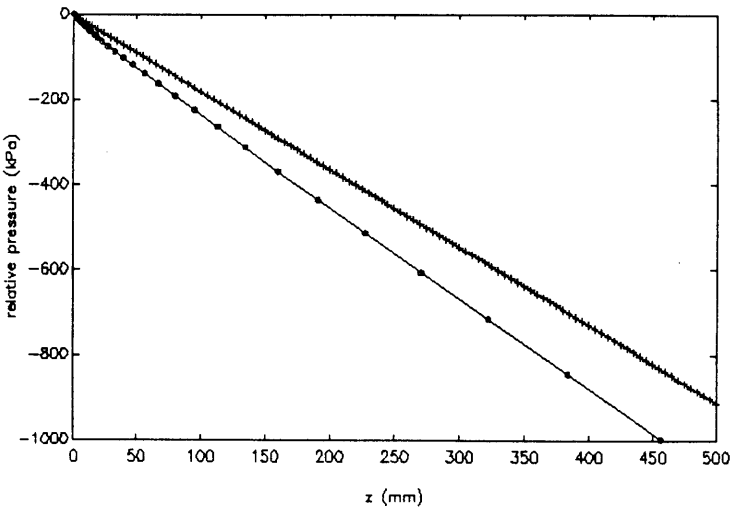

Figure 5-3. Pressures ($p - p_o$);
Unblocked Water Flow Case
—o— FLUENT
—+— hand calc

Section 6: BLOCKED WATER FLOW CASE

6.1 VELOCITY DISTRIBUTION

FLUENT calculations applied to the blocked water flow case show a double swirl existing behind the blockage, as displayed in fig 6-1:

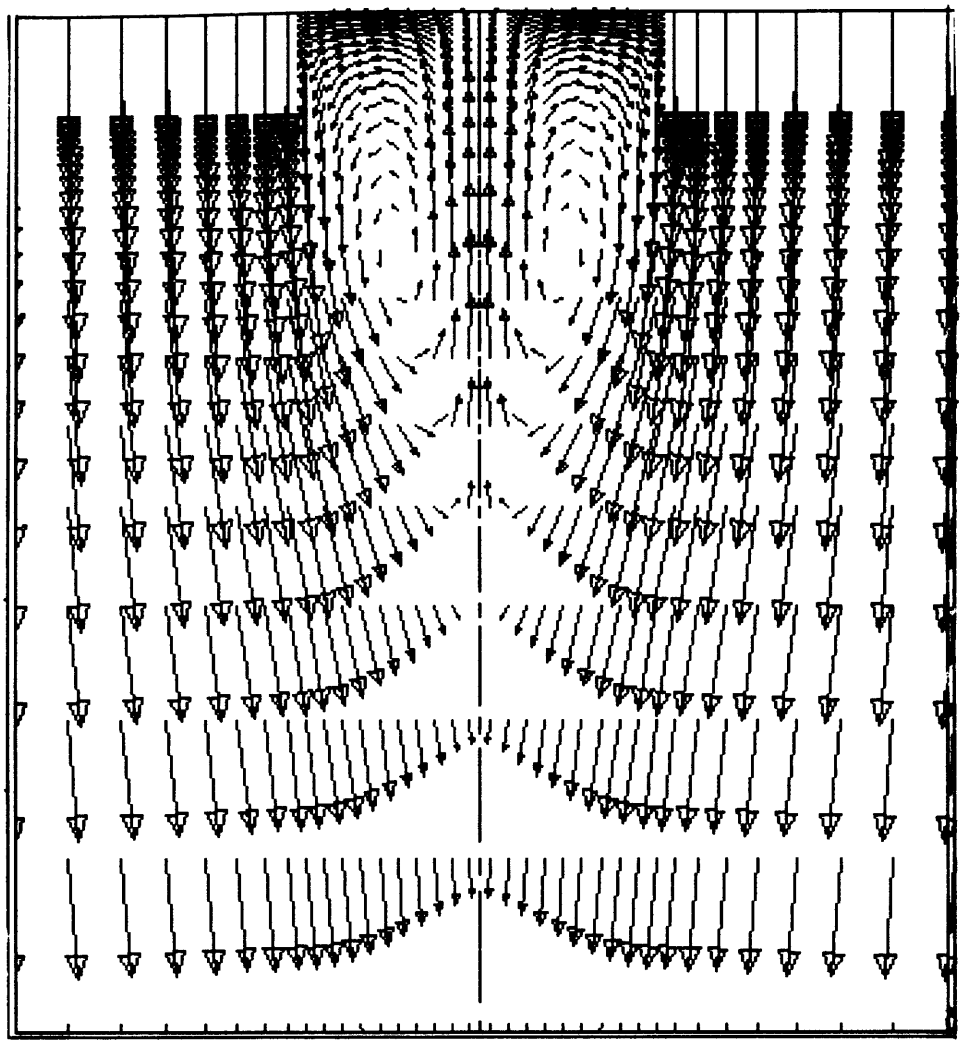

Figure 6-1. Water Velocity Vectors (from FLUENT)
Blocked Water Flow Case
y from + 11 mm to - 11 mm
z from 0 to + 24 mm

The orientation of fig 6-1 is taken from fig 2-1; that is, the z-axis (positive velocity direction) is directed downward on the page and the y-axis is directed to the left on the page.

Note that the FLUENT calculations are performed only for positive values of y. Fig 6-1 was prepared by using a symmetry print option in FLUENT. The symmetry

constraint and the stipulation of steady state implies that an even number of non oscillating swirls must be obtained for the FLUENT solution. No alternately shedding "Srouhal vortices" are possible.

The size of each swirl is roughly 4 mm by 12 mm with the center at z = + 6 mm.

6.2 TEMPERATURES

The results of FLUENT calculations of wall temperature are portrayed in figs

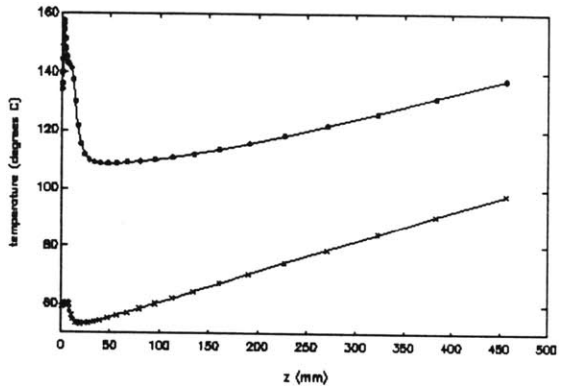

Figure 6-2. Wall Temperature and Water Temperature (x = 0); Blocked Water Flow Case (Tr 1).

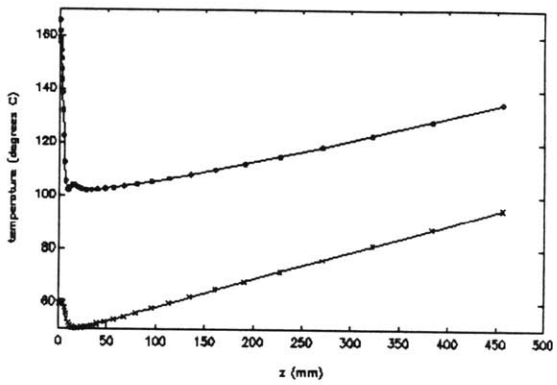

Figure 6-3. Wall Temperature and Water Temperature (x = 0); Blocked Water Flow Case (Tr 2).

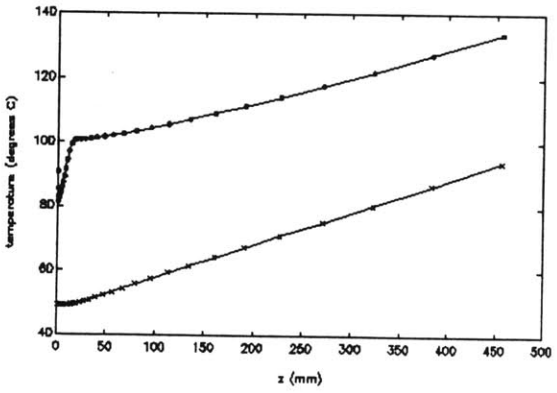

Figure 6-4. Wall Temperature and Water Temperature (x = 0); Blocked Water Flow Case (Tr 3).

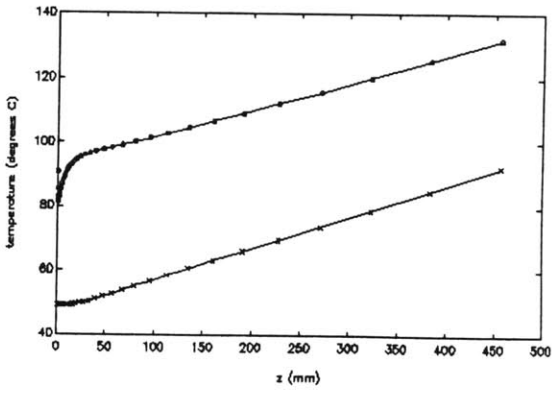

Figure 6-5. Wall Temperature and Water Temperature (x = 0); Blocked Water Flow Case (Tr 4).

6-2 through 6-5 corresponding, respectively to traverses 1 through 4. The water temperature at x = 0 is also shown for each traverse.

Traverses 3 and 4 are clear of blockage and behave in a manner similar to the unblocked case of fig 5-1. One subtlety of note is the observation that, for large z values, the traverse 4 water temperature is slightly lower than that for traverse 3. The traverse 4 wall temperature is also slightly lower than that for traverse 3.

This water temperature observation implies that a certain water temperature difference is established early in the channel and that the difference is maintained with little mixing effect at higher z values.

Traverses 1 and 2 are behind the blockage. For these traverses and for the region within the swirls (approximately 12 mm), the temperature of both water and wall are elevated above the corresponding temperatures beyond the swirls.

If we compare the relative increases to those given in figs 4-3 and 4-4 for the blocked air flow case, we see that the fluid temperatures increases are smaller in the water flow case. However, wall temperature changes are substantial, with the wall reaching about 165°C in traverse 2.

6.3 NUSSELT NUMBERS

Figure 6-6 displays Nusselt numbers for all four traverses. The values for traverses 1 and 2 are low near the channel inlet and never quite recover to unblocked values. On the other hand, traverses 3 and 4 show high entrance effect values near the channel inlet and maintain values above unblocked counterparts.

The split among Nusselt numbers near the channel exit provides evidence that water mixing is not very effective. This low mixing effect is also discussed in §6.2. In evaluating this effect, recall that the hand calculated bulk temperature is used in the Nusselt number definition (eq 4-1) and not the local fluid temperature.

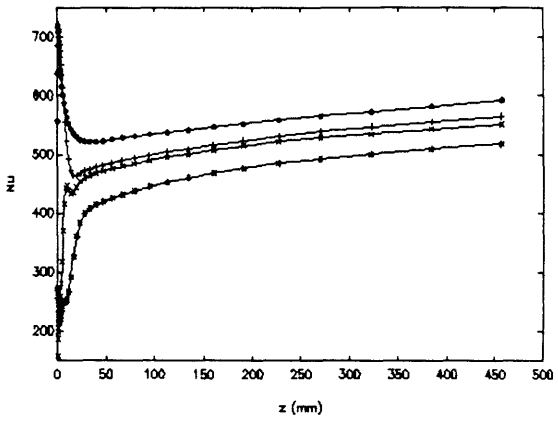

Figure 6-6. Nusselt Numbers (FLUENT) Blocked Water Flow
—*— Tr 1; —x— Tr 2
—+— Tr 2; —o— Tr 4

Figure 6-7 displays the Nusselt numbers in the region near the channel entrance to provide more detail in this region of significant divergence and significant change.

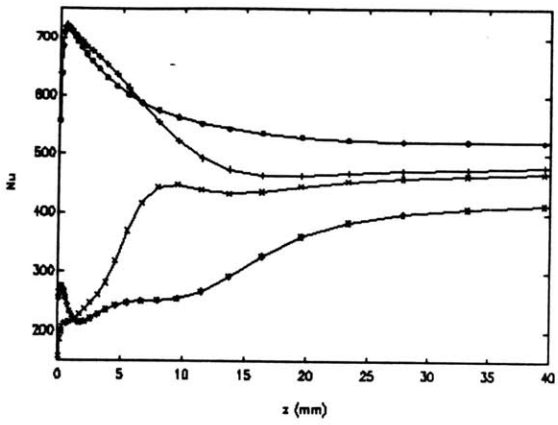

Figure 6-7. Nusselt Numbers (FLUENT) Blocked Water Flow
—*— Tr 1; —x— Tr 2
—+— Tr 2; —o— Tr 4

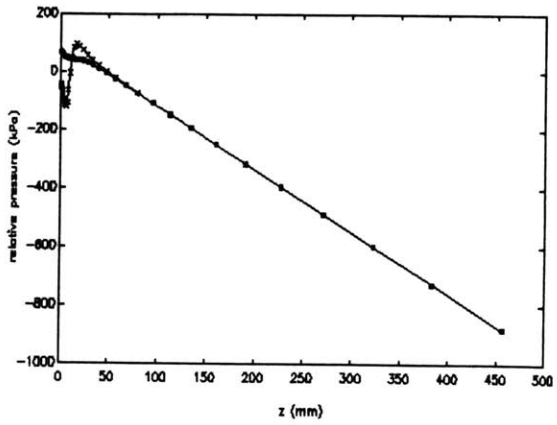

Figure 6-8. Pressure vs z; (FLUENT) Blocked Water Flow
—x— Tr 1; —o— Tr 4

6.4 PRESSURES

Axial pressure distributions from FLUENT are shown in fig 6-8 for extreme traverses (1 and 4). These distributions are similar to those for air flow in figs 4-11 and 4-12. There are dips in pressure adjacent to the swirls and humps afterward. The dip is bigger for the traverse farther into the swirl.

Note that pressures converge for the traverses as z increases. That is, the pressure becomes uniform over the cross-section at a given z-value. This is unlike the previous temperature observation. Temperature differences persist.

Section 7: DISCUSSION AND CONCLUSIONS

The findings of this study include:

- Graphs are presented that give FLUENT results for flow patterns, temperatures, Nusselt numbers, and pressures.

- FLUENT results are compared to some of the available information from the Cur air flow experiment. This comparison indicates that, in a blocked case, the FLUENT swirl is smaller and the FLUENT Nusselt number larger than observed in the experiment. However, most of the qualitative features of the experiment are correctly represented.

- FLUENT results are also presented for a blocked water flow case and for a corresponding unblocked case. In many respects, the blocked flow results appear to be analogous to those for air.

- A real benefit comes from the act of attempting to understand details of the FLUENT output. The act sharpens intuition about the significant processes in blocked flow heat transfer.

One of the heat transfer processes of interest is the elevation of fluid temperature inside a swirl. The elevation occurs from the need to remove added heat from a stationary swirl by lateral eddy conduction. A larger swirl as present in the experiment implies the need for a higher swirl temperature to achieve the needed conduction. In addition, since it is important to get a good eddy conduction treatment, there are extra demands on the accuracy the turbulent modeling.

One of our intents had been to explore other mesh structures, other convergence approaches, other turbulence models, and other physical cases. These alternatives are available with FLUENT. However, the process of getting, and interpreting, correct timely solutions for each of the four cases of this report proved to be very difficult. Late software, slow convergence, and computer difficulties implied that only a few cases could be studied. A much faster turnaround is essential to complete a study with more breadth.

Our FLUENT calculations, hand calculations, and Cur interpretations were done partly in sequence but also partly in parallel. For example, the hand calculations for pressure drop in the air flow cases were complete before we had adopted the heated effect term in eq 3-9. We judged that this term was close enough to unity to justify retaining the earlier results with no heating effect. In the other known cases of inconsistency, we judged the effects to be minor and the report conclusions to be unaffected.

Finally, the FLUENT results to date are of continuing interest. We infer that, with a wider range of blocked results and with additional confirmatory experiments, software similar to FLUENT can be used as a basis for extended design calculations.

REFERENCES

B-1 R.D. Blevins, "Applied Fluid Dynamics Handbook," Van Nostrand Reinhold, New York, 1984.

C-1 N. Cur, "Local Turbulent Heat Transfer Coefficients in a Symmetrically or Asymmetrically Heated Flat Rectangular Duct with Either Uniform or Nonuniform Inlet Velocity," Univ of Minnesota PhD Thesis, Mar-82.

D-1 T. Dormer, Jr., "Pressure Drop with Surface Boiling in Small-Diameter Tubes," MIT SM Thesis, Sep-64.

F-1 "FLUENT User's Manual," Version 3.0, creare.x Inc., Hanover NH, Mar-90.

H-1 J.O. Hinze, "Turbulence: An Introduction to its Mechanism and Theory," 2nd ed, McGraw-Hill, New York, 1975.

K-1 J.H. Keenan et. al., "Steam Tables," Wiley-Interscience, New York, 1978.

K-2 J.H. Keenan, J. Chao, and J. Kaye, "Gas Tables; International Version; Thermodynamic Properties of Air Products of Combustion and Component Gases Compressible Flow Functions," 2nd ed., Wiley-Interscience, New York, 1983.

P-1 M. Pichal and O. Sifner, "Properties of Water and Steam," Proceedings of the Eleventh International Conference, Hemisphere Publishing, New York, 1989.

R-1 W.M. Rohsenow, J.P. Hartnett, and E.N. Ganić, eds., "Handbook of Heat Transfer Fundamentals," 2nd ed., McGraw-Hill, New York, 1985.

S-1 E.M. Sparrow and N. Cur, "Maldistributed Inlet Flow Effects on Turbulent Heat Transfer and Pressure Drop in a Flat Rectangular Duct," Trans. Am. Soc. Mech. Engrs. J. Ht. Transfer, 105, 527-535 (1983).